Experimental Platform to Facilitate Novel Back Brace Development for the Improvement of Spine Stability

L. Cooper[1], A. Gullane[1], J. Harvey[1], A. Hills[1], M. Zemura[1], J. Martindale[2], A. Rennie[1], D. Cheneler[1]

[1]Engineering Department, Lancaster University, Lancaster, LA1 4YW, UK

[2]Wrightington Wigan and Leigh NHS Foundation Trust, Wigan, WN1 2NN, UK and Lancaster University Health Hub, Lancaster University, Lancaster, LA1 4YG, UK

The spine or 'back' has many functions including supporting our body frame whilst facilitating movement, protecting the spinal cord and nerves and acting as a shock absorber. In certain instances, individuals may develop conditions that not only cause back pain but also may require additional support for the spine. Common movements such as twisting, standing and bending motions could exacerbate these conditions and intensify this pain. Back braces can be used in certain instances to constrain such motion as part of an individual's therapy and have existed as both medical and retail products for a number of decades. Arguably, back brace designs have lacked the innovation expected in this time. Existing designs are often found to be heavy, overly rigid, indiscrete and largely uncomfortable. In order to facilitate the development of new designs of back braces capable of being optimised to constrain particular motions for specific therapies, a numerical and experimental design strategy has been devised, tested and proven for the first time. The strategy makes use of an experimental test rig in conjunction with finite element analysis simulations to investigate and quantify the effects of back braces on flexion, extension, lateral bending and torsional motions as experienced by the human trunk. This paper describes this strategy and demonstrates its effectiveness through the proposal and comparison of two novel back brace designs.

Keywords: additive manufacturing, back braces, spine, finite element analysis, medical design

Introduction

The single largest cause of disability internationally is back pain, with lower back pain having a prevalence of 9.4% globally (Hoy, et al., 2014). This has a significant economic impact with 149 million working days lost per year globally due to lower back pain (Office for National Statistics, 2017). The modern way of life is a major contributing factor, with poor posture, an aging population and a sedentary lifestyle all leading to an increased risk (Morl & Bradl, 2013) (Woolf & Pfleger, 2003). Similarly, there exists a plethora of medical conditions affecting the spine (Woolf & Pfleger, 2003).

Whilst some conditions benefit from free movement, others benefit from constraint to support the back and reduce pain. For instance, back braces limit the motion of the spine to stabilise weak, injured or fractured vertebrae and prevent progression of spinal deformity (Hawkinson, 2016) (Kawaguchi, et al., 2002). The extent of motion restriction could be of great interest and importance. Current brace designs can reduce trunk motion sufficiently to prevent pain or further injury for the prescribed recovery time whilst allowing the wearer to carry out some thoracolumbar motion (Cholewicki, et al., 2007). Where designs fall short is in restricting specific trunk motion, i.e. restriction limited just to lateral bending, for instance. As some musculoskeletal back conditions actually benefit from movement (Longo, et al., 2012), targeted restriction, as compared to gross restriction, deserves further investigation.

In addition, prolonged wear of rigid back braces can lead to substantial muscle mass loss due to reliance on the brace to impede motion (Eisinger, et al., 1996). Current designs restrict muscle recruitment in brace conditions inducing further problems for the patient. Research into soft braces largely indicates no modification to abdominal and trunk muscles if the prescribed wearing period is adhered to (Fayolle-Minon & Calmels, 2008) (Cholewicki, et al., 2010). The inverse relationship that exists between the extents of muscle restriction against comfort of the brace attributes to the difficulty in gauging the effect of prolonged wear of rigid braces (Hsu, et al., 2008).

Two methods of measuring motion of the spine are employed in the literature and subsequently can be applied to test the effectiveness of back braces: biomechanical models (Ivancic, et al., 2002), and through electromyography (EMG) data from live healthy subjects in brace conditions (Cholewicki, et al., 2007) (Cholewicki, et al., 2010) (Lariviere, et al., 2014). Cholewicki *et al.* (Cholewicki, et al., 1995) conducted experiments on subjects in the upright standing posture position and performed near maximal ramp contraction, which is the body moving from rest to the maximum angle it can bend in flexion, extension and lateral bending, in each case checking the extent of muscle recruitment of torso muscles for spine stability. However, due to ethical issues with regards to access of patient data or use of live subjects, no current reliable methods exist to test the effectiveness of back braces. This research aims to address the shortcomings of the current design process and provide a method of assessing back braces quantifiably.

In this work, the design and operation of an experimental test rig for the quantified design, comparison and optimisation of back braces is described, hence providing a method for the braces to be more easily and ethically tested. The test rig incorporates an artificial spine and torso, shown here to be mechanically equivalent to a human torso. In order to prove its effectiveness, two novel back brace designs have been tested on the rig. It has been shown that by using the test rig, it is possible to quantify the reduction in flexion, extension, lateral bending and torsion.

The test rig, including spine, torso and brace design have been modelled using finite element analysis (FEA). This analysis allows for the study of spine motion during brace development. Through comparison to studies found in the literature, the validation simulations presented show that the simplified geometry, constraints and engineering materials used here have a mechanical response similar to equivalent components found in the human torso. Many complex FEA models of the spine exist, however only particular segments relevant to the area of study are usually created, hence the movement of a detailed full spine model has never been fully investigated in FEA (Huynh, et al., 2012) (Carboni & Dal Pozzo, 2017), especially with the consideration of the full torso and many of the soft tissue therein. However recent advances in complete musculoskeletal models of the human spine in multibody dynamic simulations, which could be incorporated into FEA models, should be noted (Bayoglu, et al., 2019). The spine material models employed throughout previous work varies tremendously, with the intervertebral discs often modelled as simple cylinders between spinal vertebrae (Kurutz, 2010). It is common to split the vertebrae into both cortical and cancellous bone, and the intervertebral discs into nucleus pulposus and annulus fibrosus sections. Additionally, ligaments are commonly found within FEA spine models and the muscle systems seldom modelled. Here, a FEA model of the spine and torso is described and it is shown how these simulations can facilitate back brace development.

Methods

Experimental Rig Design

The artificial spine and torso used on the test rig was developed using FEA to ensure it was mechanically equivalent to a human torso. The spine geometry developed was that of an average adult male. Dimensions were found through analysing studies undertaken by Panjabi *et al.* (Panjabi, et al., 1992), who used CT scans of a cadaver to determine the curvature of the spine and quantitatively describe the surface anatomy of 60 lumbar vertebrae. A simplified computer-aided design (CAD) model, shown in

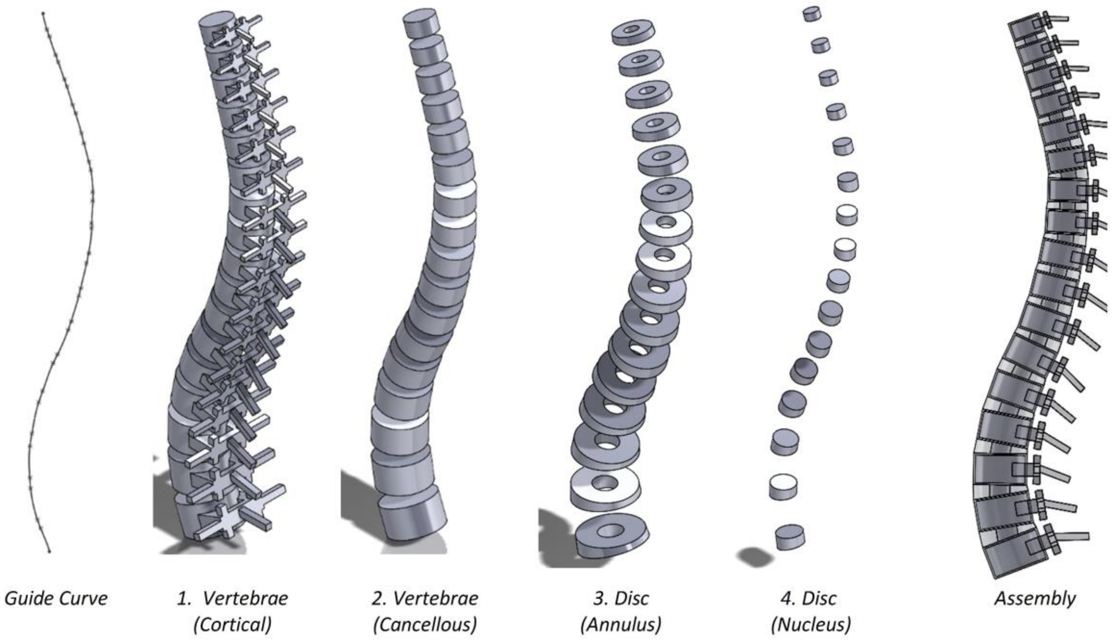

Figure 1, was then created for use within the study.

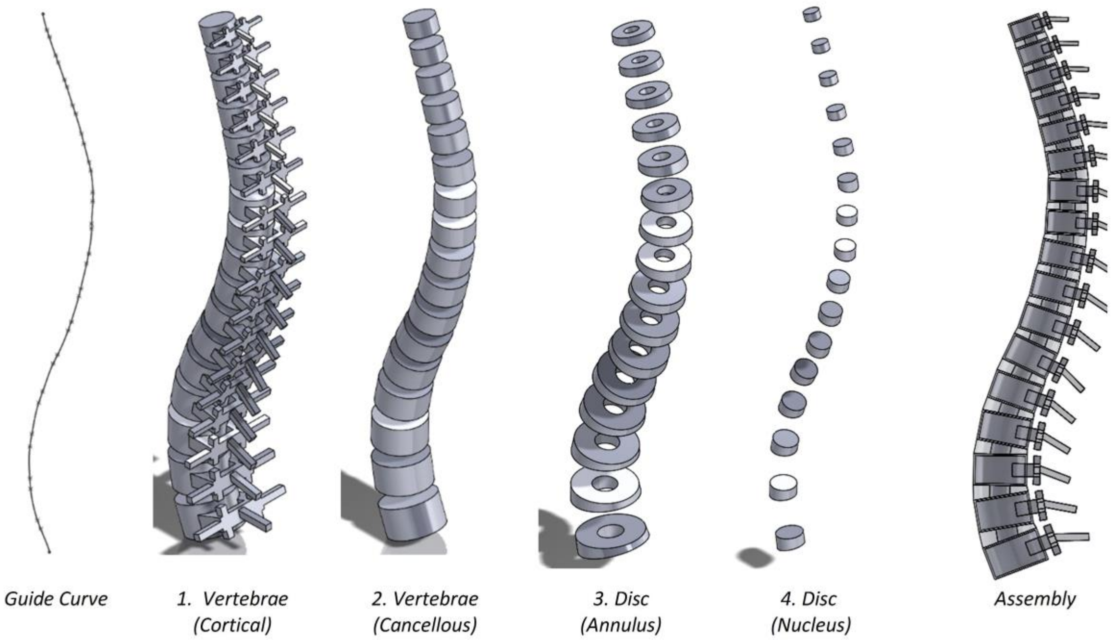

Figure 1 - Breakdown of parts present within the spine CAD model

The CAD assembly permitted the breakdown of the spine into its constituent parts, which allowed separate material models to be applied to each. The Mooney-Rivlin two-parameter model was chosen to represent the discs, a model which predicts the behaviour of hyperelastic materials through curve fitting to data and used in numerous past studies (Gómez, et al., 2017) (Wagnac, et al., 2011) (Schmidt, et al., 2006) (Dreischarf, et al., 2014). The elastic modulus of vertebrae ranges from 1.5 to 3 GPa (Swamy, 2014), and so ABS1400 with an Young's modulus of 1.68 GPa (Ultimaker, 2017) was selected to represent bone within the spine structure. Ligaments were modelled as tension-only springs and defined through a particular stiffness (Pitzer, et al., 2016). Compressive testing of flexible polyurethane foam samples yielded an elastic modulus of 0.128 MPa, within the limits stated by Bonnaire *et al.* (Bonnaire, et al., 2014) for the human abdomen (0.01 to 1 MPa). Due to the suitable elastic modulus, low cost and ease of use, it was selected to represent body mass and soft tissue within the test rig torso.

Table 1 provides a breakdown of the material properties.

Table 1 - Material property data

Part	**Material Model**	**Modulus [MPa]**	**Poisson's Ratio ν**	**Reference**
Accurate Model				
Cortical Bone	Linear Isotropic	5000	0.3	(Rohlmann, et al., 2006)
Cancellous Bone	Linear Isotropic	10	0.2	(Kurutz, 2010)
Annulus Fibrosus	Mooney-Rivlin	C1=0.14, C10=0.56, D=0.143		(Gómez, et al., 2017)
Nucleus Pulposus	Mooney-Rivlin	C1=0.03, C10=0.12, D=0.067		(Gómez, et al., 2017)
Ligaments	Spring Elements			(Pitzer, et al., 2016)
Test Rig				
ABS1400 (Vertebrae)	Linear Isotropic	1681.5	0.3	(Ultimaker, 2017)
Soft Polyurethane Foam (Torso)	Linear Isotropic	0.128	0.3	
Hard Polyurethane Foam (Discs)	Linear Isotropic	5	0.3	(Seo, et al., 2013)

In order to benchmark the effect of the geometry and constraints in the artificial spine model used here against that of an actual human spine, the maximum displacement of the L2, L3 and L4 vertebrae were examined using the mechanical properties of human tissue and compared against studies undertaken by Wang *et al.* (Wang, et al., 2006). In that study, and replicated here, a moment of 10 Nm was applied upon the superior surface of the L2 body, and the inferior surface of the L4 body was fixed. This is the maximum load that the spine can withstand before any spinal injury is caused (Yamamoto, et al., 1989). Each loading condition is displayed in

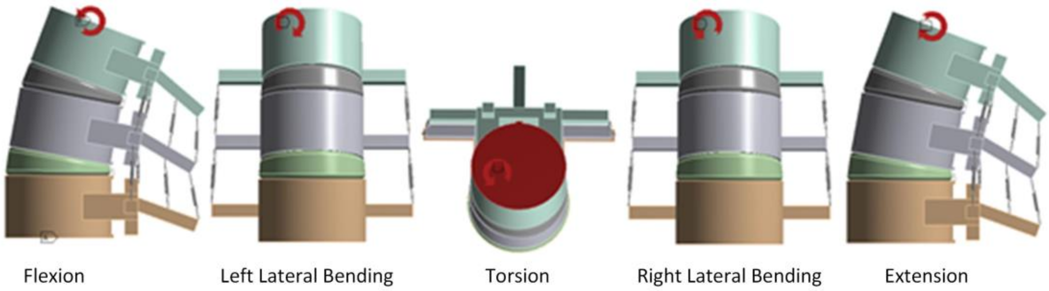

Figure 2

and the comparative results given in Table 2. The data shows that there is a reasonable equivalency in the mechanical response between the geometry and constraints used in the spine model here and those found in an actual human spine.

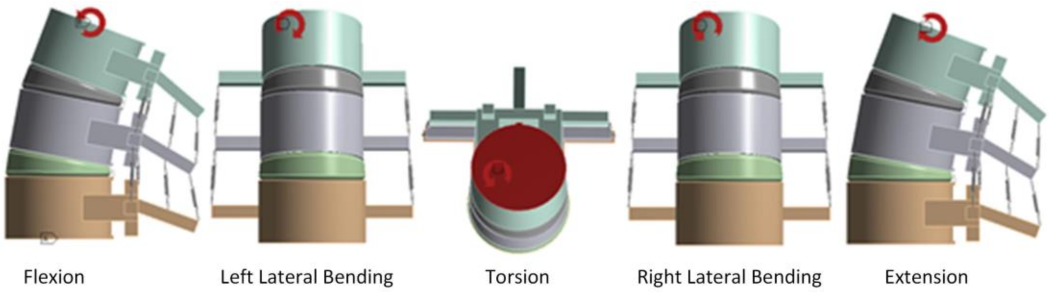

Figure 2 - L2-L3-L4 Loading and boundary conditions

Table 2 - Simulation 2 results summary

	Flexion	**Extension**	**Left Bending**	**Right Bending**
L3 Displacement (mm)	1.8272	1.263	2.8389	2.8355
Literature Value (mm) (Wang, et al., 2006)	1.66	0.97	3.27	3.27

Given this data, it can be seen that even with the simpler geometry used within the test rig, the spine is still undergoing equivalent motion. To ensure the engineering materials used in the test rig are suitable, the materials properties in the simulation were changed to that of ABS and polyurethane foam, as used in the test rig. The data was compared to the model previously described, which used the properties of human tissue so that it could be verified that the materials being used were mechanically equivalent. A close match is seen in Figure 3, highlighting how the materials and geometries used within the test rig are a suitable choice. Again, the springs shown represent the tension-only spring elements that model the ligaments.

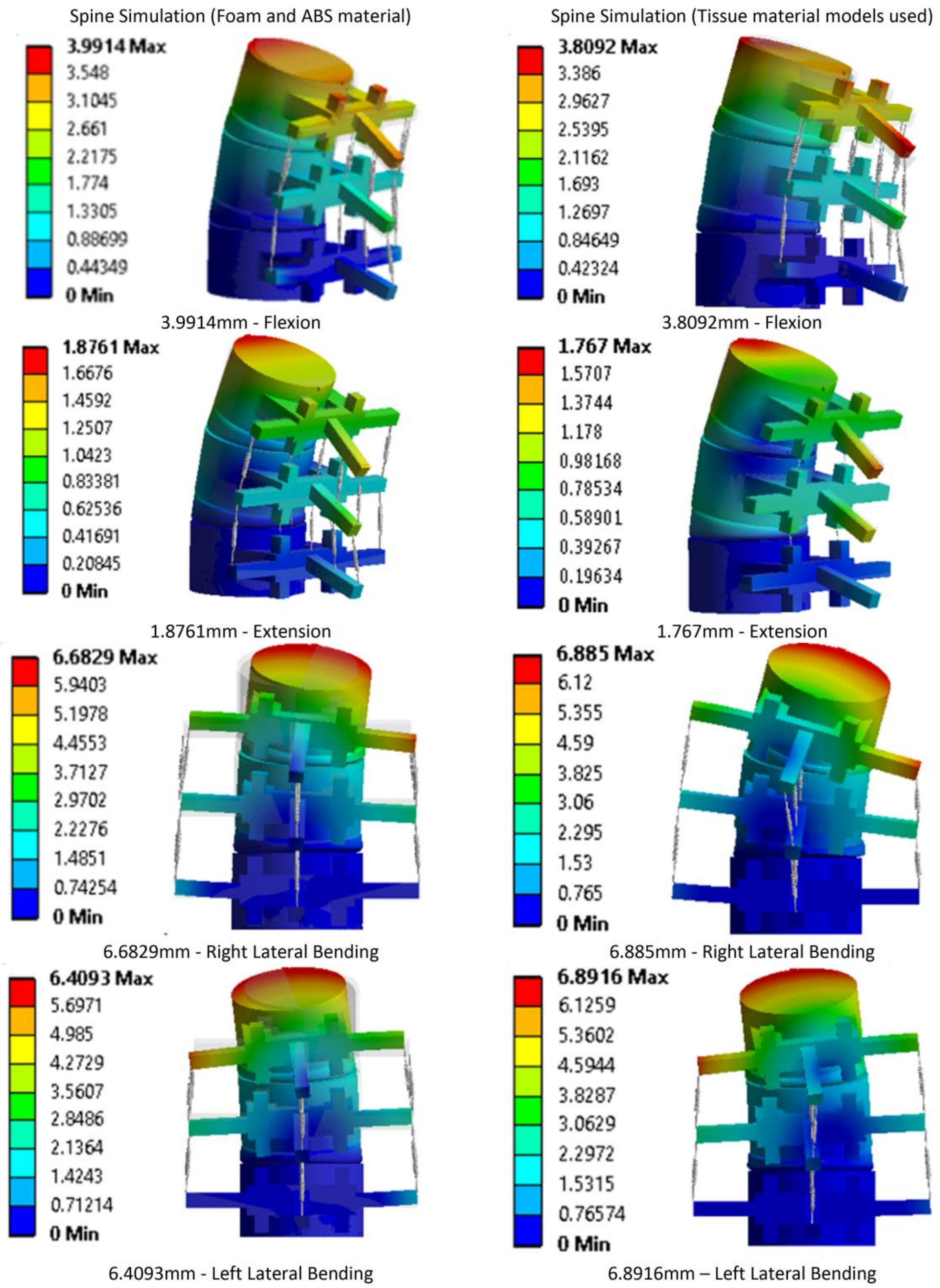

Figure 3 - Total L2-L3-L4 displacement comparisons

To investigate the mechanical behaviour of the full torso, the spine was added to a torso CAD model. Multiple cross-sectional dimensions were taken from a human torso mannequin to achieve the required external geometry, as shown in

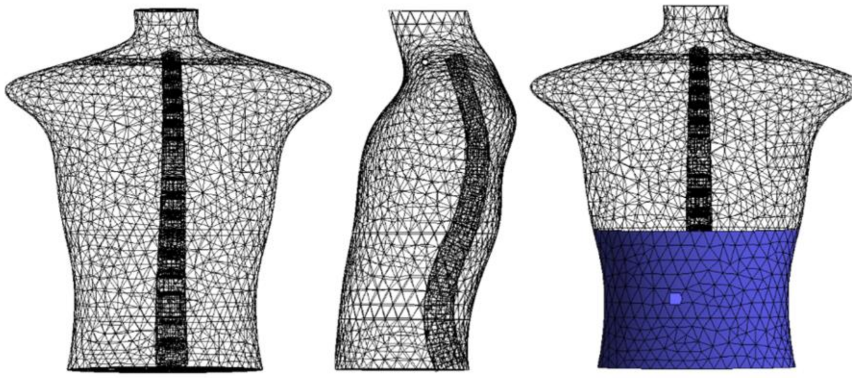

Figure 4.

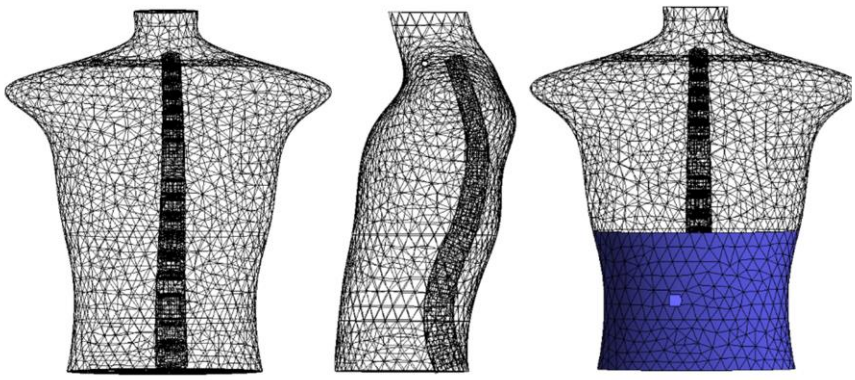

Figure 4 - Torso and spine CAD model. The figure on the right shows the position of a hypothetical back brace in blue. This was modelled as an elastic foundation for initial design purposes.

The final step for verifying the effectiveness of the simulated torso was to show how a simple back brace around the waist achieves a reduction in the range of motion.

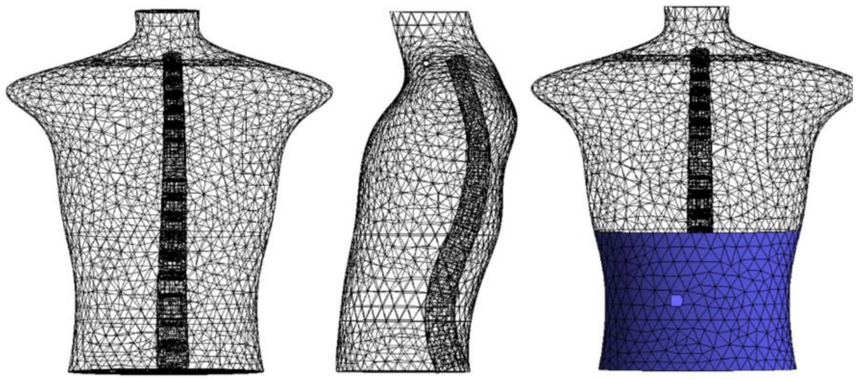

Figure 4 shows the sectioned area where a back brace would impart a pressure on the torso. The elastic support boundary condition provides a stiffness normal to the surface it is applied on and is defined through a foundation stiffness. This stiffness is defined as the pressure required to produce a unit of normal deflection (ANSYS, 2017) and thus is representative of an elastic brace being worn.

A normal load of 58.4 N was applied to the sternum, to be consistent with later experiments and to simulate the spine and torso displacement during flexion. Foundation stiffness was incrementally increased and both maximum displacement and lumbar displacement analysed (

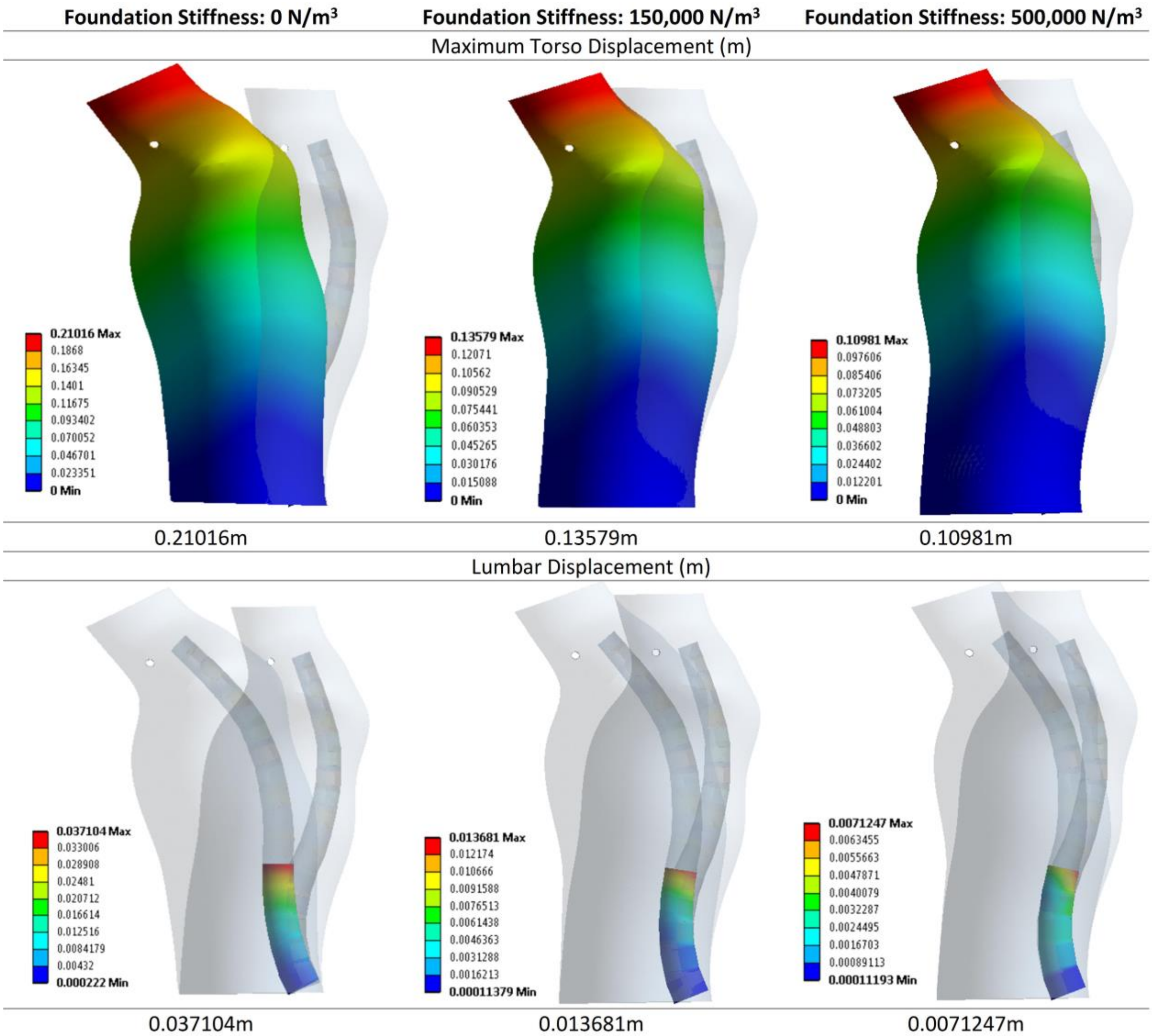

Figure 5). It can be seen that through increasing the pressure around the waist, a reduction in the total displacement of the torso is possible. It is also noted that the reduction in displacement is more evident in the lumbar region. It is postulated that data such as that derived from

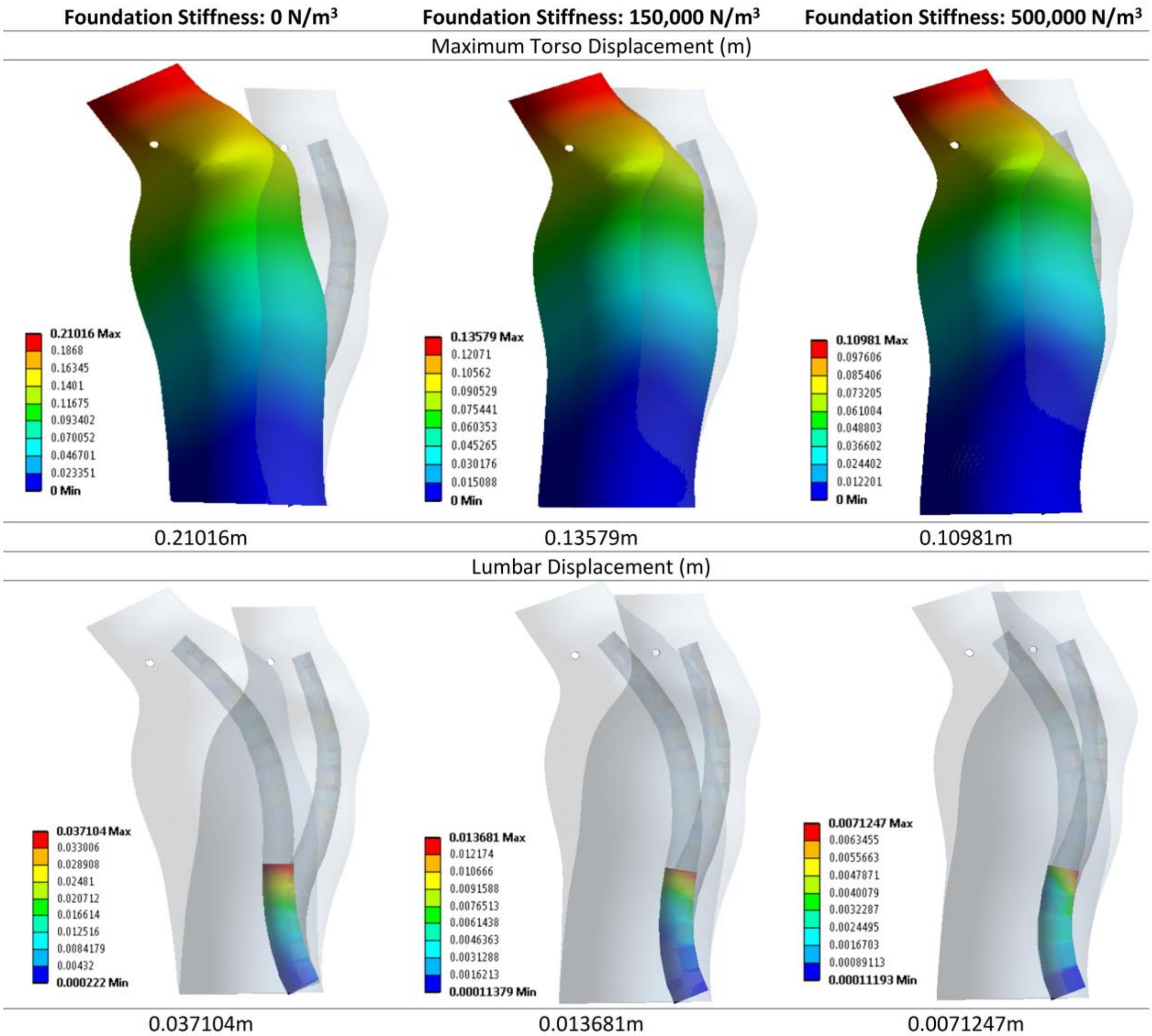

Figure 5 may be used to tune or design a back brace to a desired range of motion.

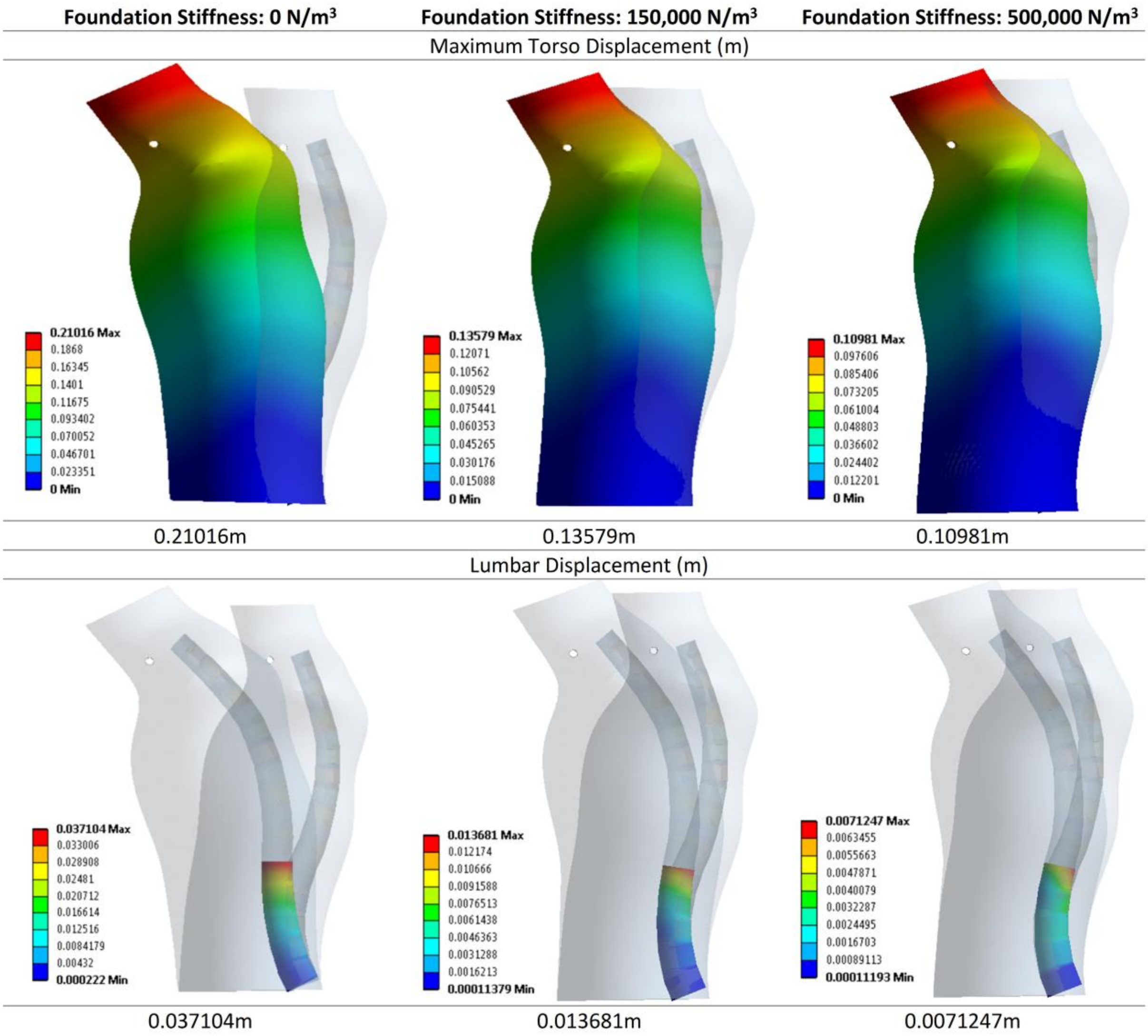

Figure 5 - Braced foam torso displacement

Test Rig Fabrication

The test rig comprises two fundamental features: an artificial mechanically equivalent human torso, and a frame mechanism designed to manipulate the torso into flexion, extension, lateral bending and torsional motions. Unlike the FEA models, the fabricated vertebrae were treated as a single material structure to aid in manufacture. This does not affect the mechanical behaviour of the torso. Such a structure lends itself to fused deposition modelling (FDM; an additive manufacturing process), a method well suited to fabricating the unique geometries of vertebrae, and hence the method adopted in this instance. All vertebrae, ribs and sternum were additively manufactured using FDM on a Ultimaker 2 (Ultimaker-Geldermalsen, Netherlands) with a 0.4 mm nozzle. A 3mm diameter ABS1400 feedstock and a nozzle temperature of 240 °C was used (build plate temperature was 80 °C). All intervertebral discs were cast as one collective piece of medium density polyurethane foam (Polycraft 022-medium foam; from MB Fibreglass), in a two-part mould fabricated using FDM. This piece was then cut to the correct geometries in sections using a scalpel.

The ribcage contributes to a reduction in flexibility in the torso and an increase in motion stability [27]. The ribcage was designed based on cadaver data of an average male, combined with reverse engineering of existing skeletal models (Panjabi, et al., 1992). Simplifications were made to the geometry of the ribs and sternum to improve the quality of the parts produced using FDM. To further simplify the ribcage design, only essential ribs were included. These include ribs necessary for load distribution. Only four rib pairs were therefore included in the design, connected to vertebrae T1, T3, T5 and T10. The ribcage was also fabricated from ABS1400 to simulate bone within the spinal structure. The assembled CAD model of the artificial spine is shown in

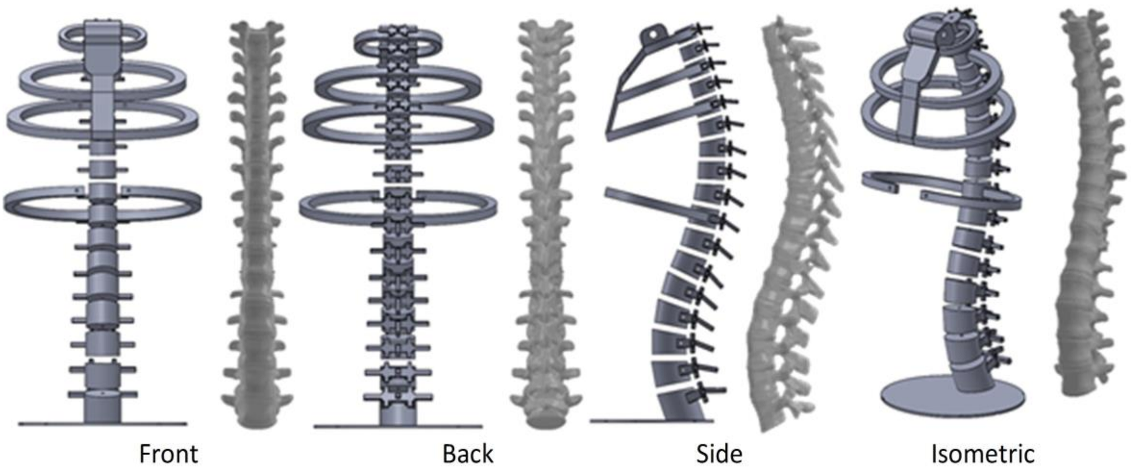

Figure 6 and compared directly to CT scan data. This CT scan data was retrieved from an open access source (An, 2014) which used Materialise Mimics software (Materialise, 2018) to convert CT slices into a solid model. Radiographic data was taken from a male cadaver without any apparent spine trauma or pathological effects. The data is used here purely for visual comparison.

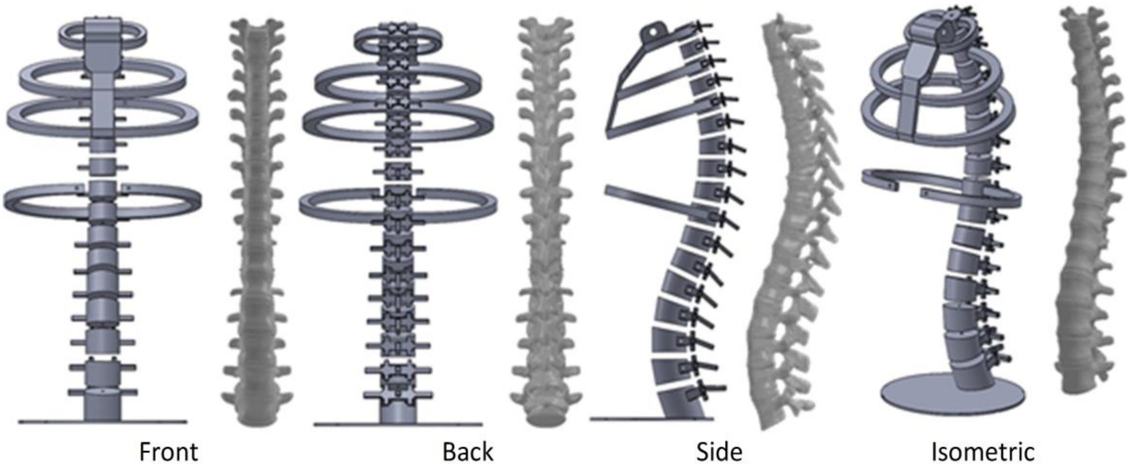

Figure 6 - Spine CAD assembly compared with CT scan data of example human spine

The test rig comprises a steel framework featuring a set of pulley systems capable of manipulating the torso (

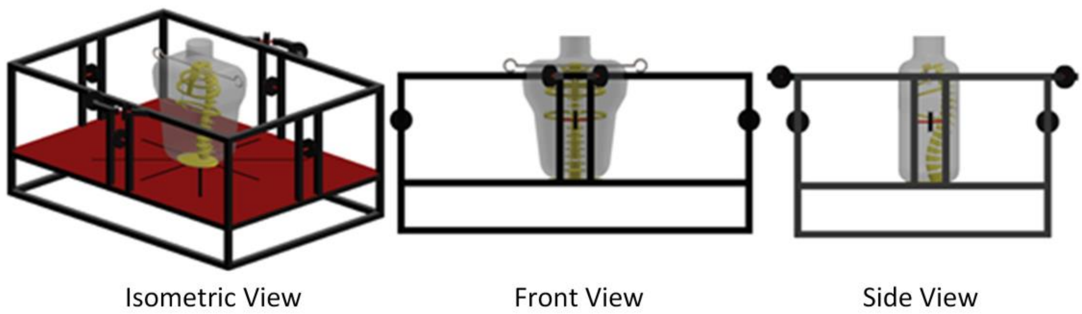

Figure 7). A steel rod connected to the sternum and protruding from the torso acts as the shoulders and provides a connection point for the cables attached to the pulley wheels. The front/back/lateral pulley wheels are lowered in line with the upper abdominals/obliques/lower back in order to generate true anthrompomorphic motion in flexion/extension/lateral bending. Since torsional motion is greatest at the top of the thoracic spine, and progressively less lower

down the spine, the torsional motion is created in line with the T1 vertebra. The geometry of the torso was obtained by creating a mould around a torso mannequin using Plaster of Paris.

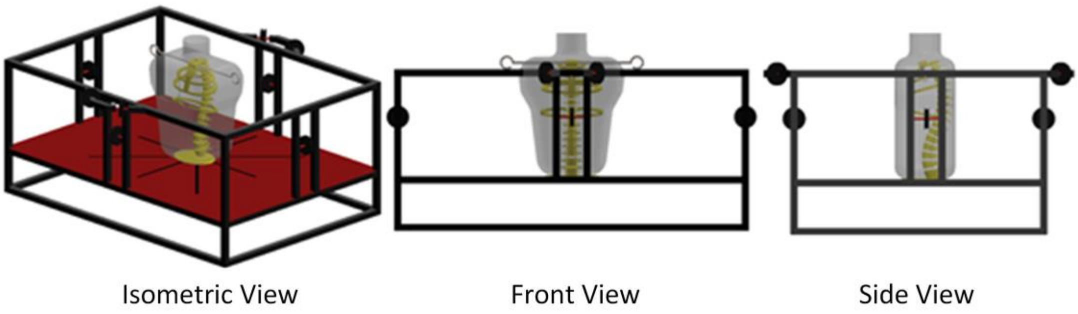

Figure 7 - Test rig CAD assembly

Test Rig Test Method

The intention of the test rig is to quantify and compare the reduction in motion caused by the presence of various brace designs. Three methods were used to record respective motion displacement: flex sensors attached along the centre of the torso recording bend angle of the torso; image analysis of photographs taken from fixed locations both before and after applying load (see

Figure 8); and manual measurement of the displacement of a fixed point on the shoulder rod from the horizontal plane.

All three methods were used in recording flexion/extension/lateral bending; however, torsion does not lend itself to use of flex sensors or manual displacement measurement, and hence relies solely on imaging. A preliminary range of motion test was undertaken on the rig and validated using the FEA (see

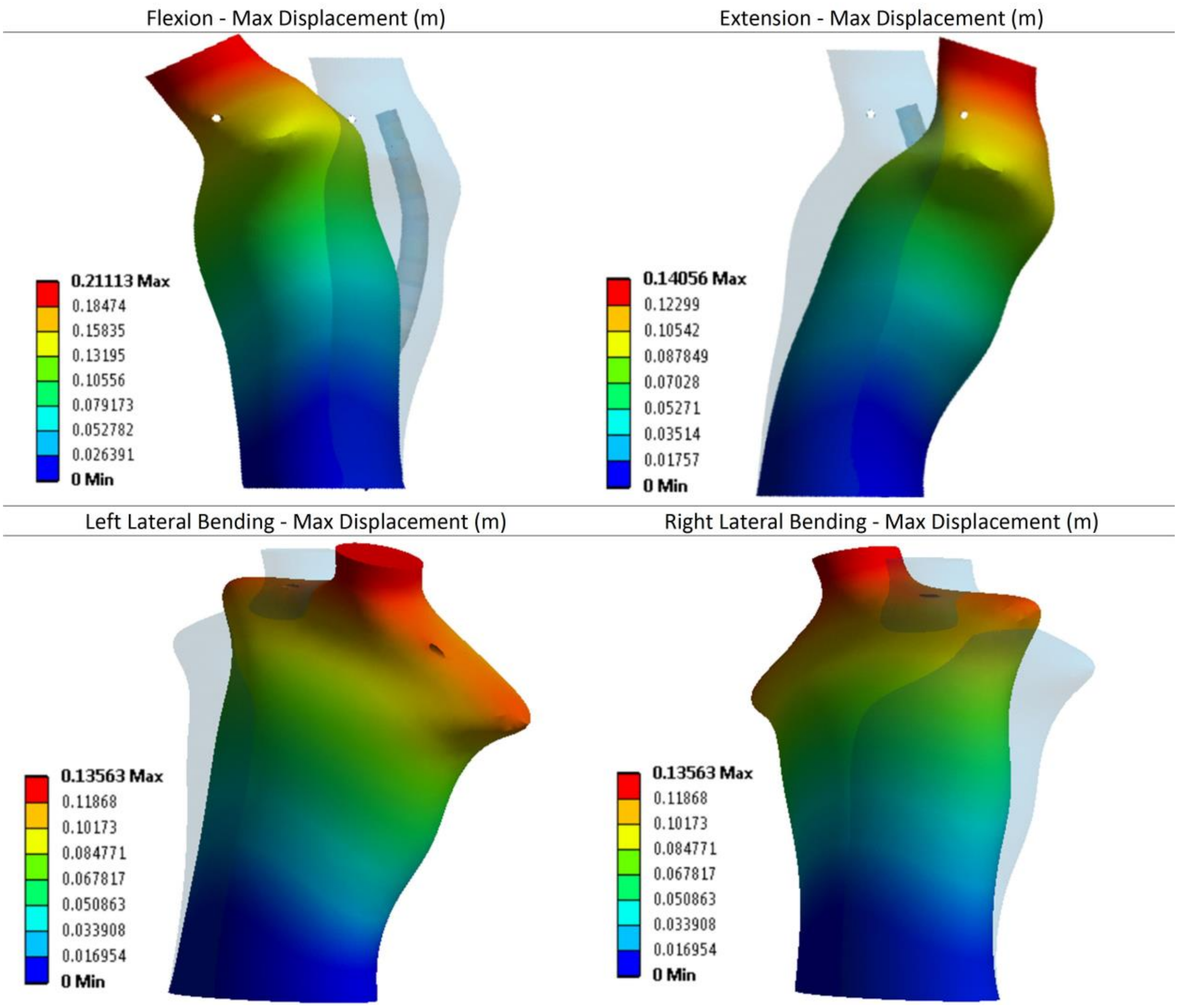

Figure 9) model described above, and a summary of the key results obtained is given in Table 3. Load was applied to achieve a desired range of motion and the same applied on both the mechanical rig and in simulations to provide the basis for fair comparisons.

Table 3 - Test rig range of motion results

	Flexion	Exte
Mass Applied (Kg)	5.95	3.

Max Displacement (mm) in Experiment (	199.1	16

Figure **8**)

Max Displacement (mm) in Simulation (	211.1	14

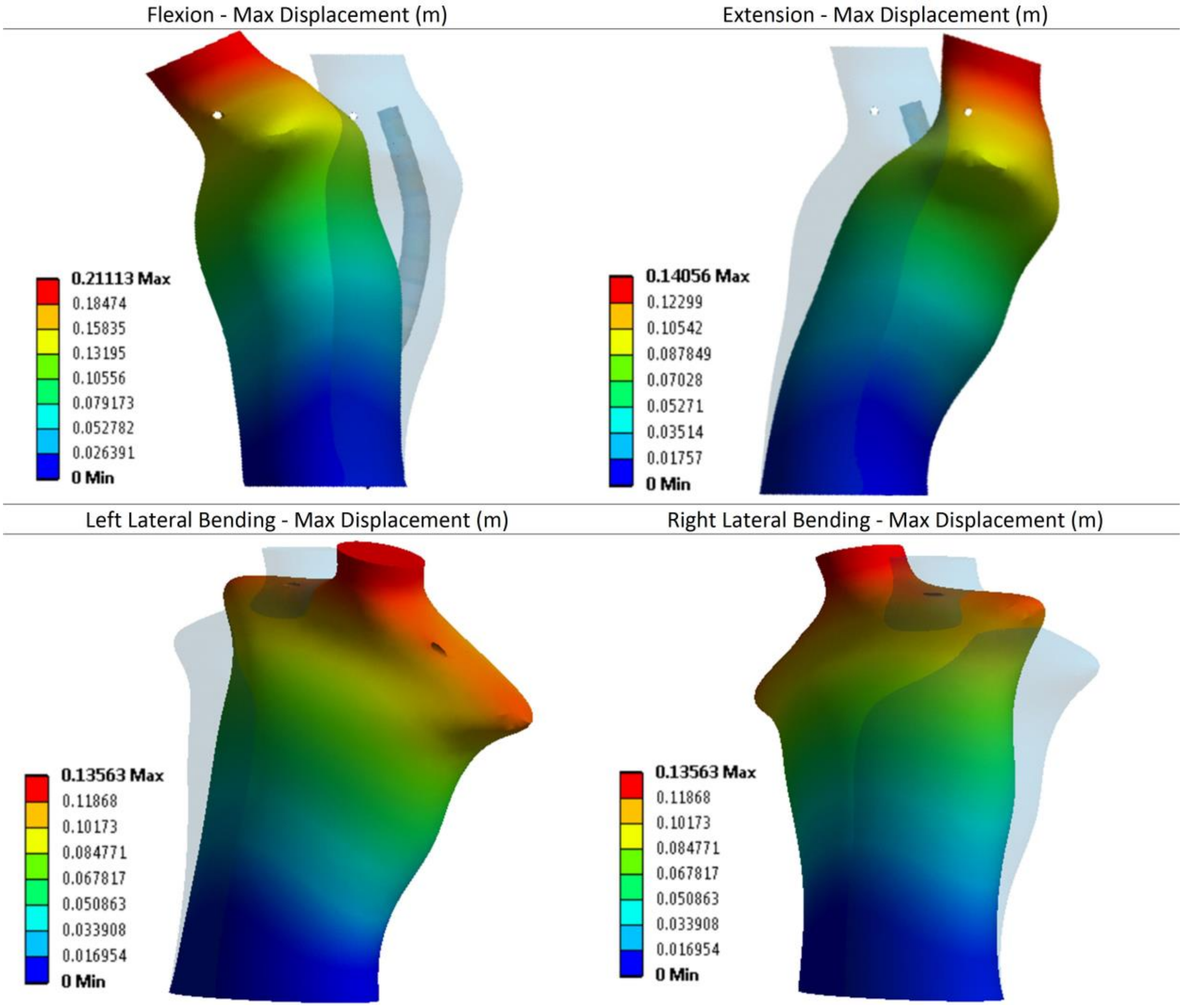

Figure **9**)

247

Figure 8 - Test rig torso motions given loadings stated in Table 3

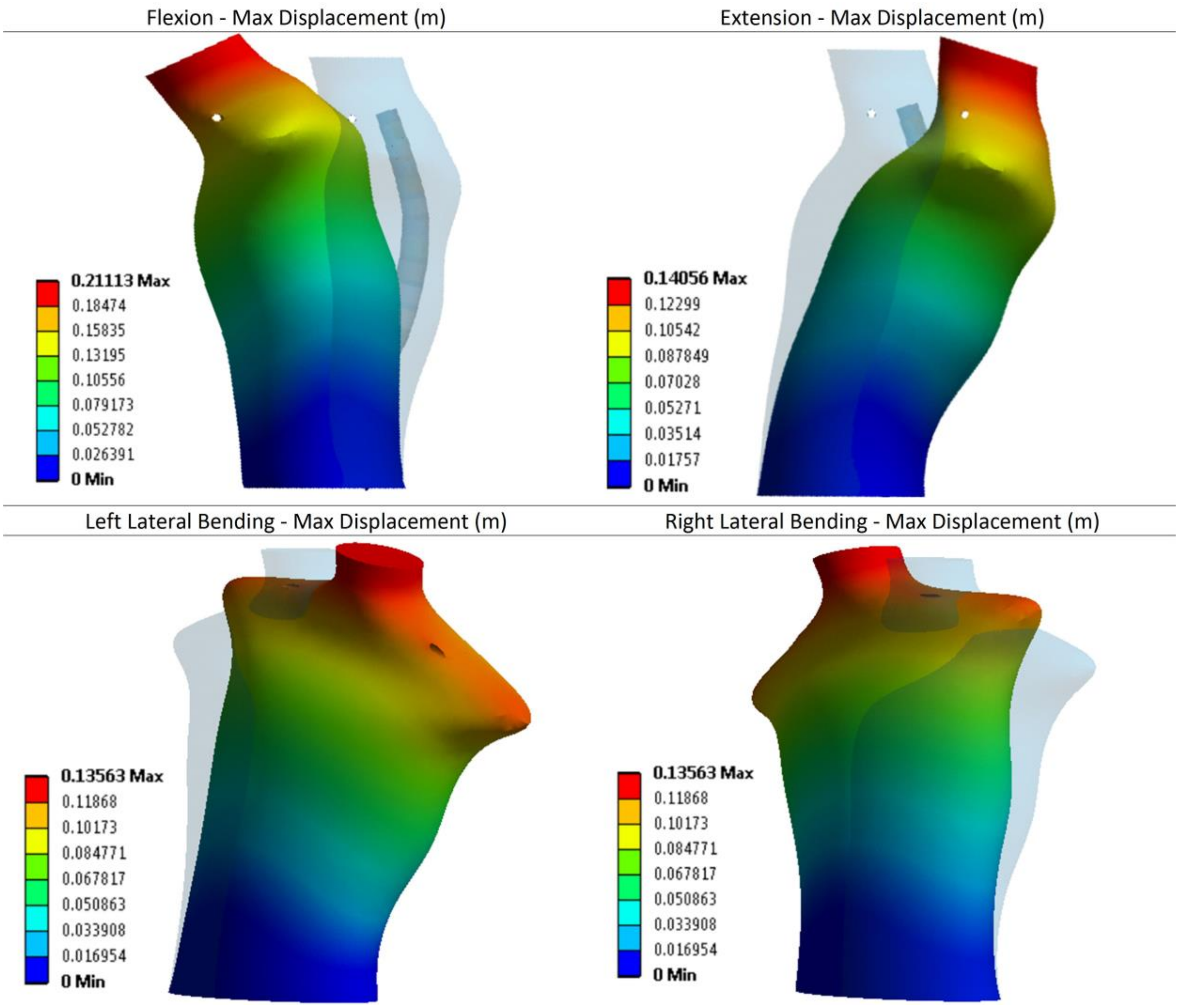

Figure 9 – Simulated torso displacements for comparable loadings as test rig shown in

Figure 8

Brace Design

The first back brace design utilised a combination of topologically customised shoulder pads and unidirectional chain links (

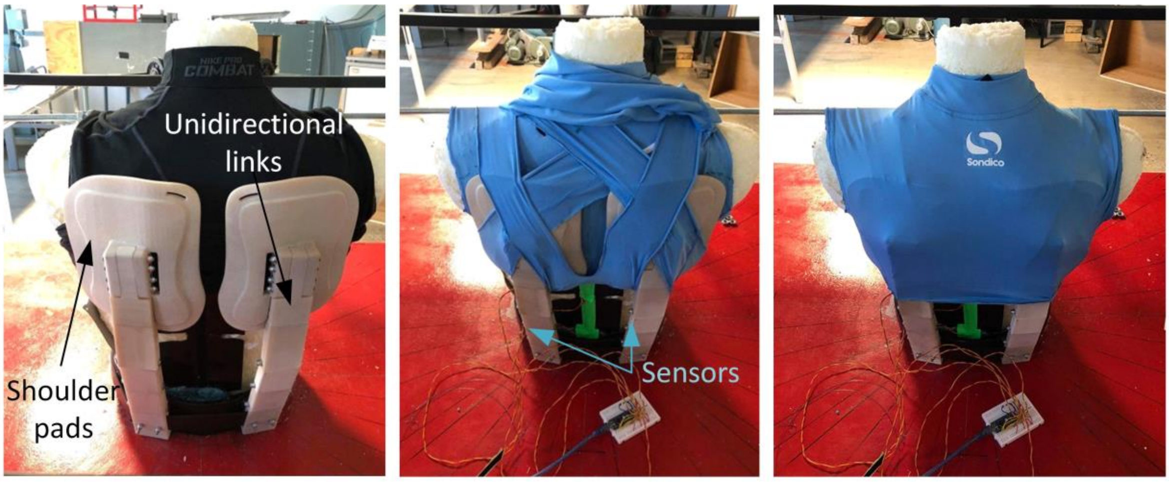

Figure 10). The design intent of this concept was to allow flexion while restricting extension, lateral bending and torsion to a noticeable degree.

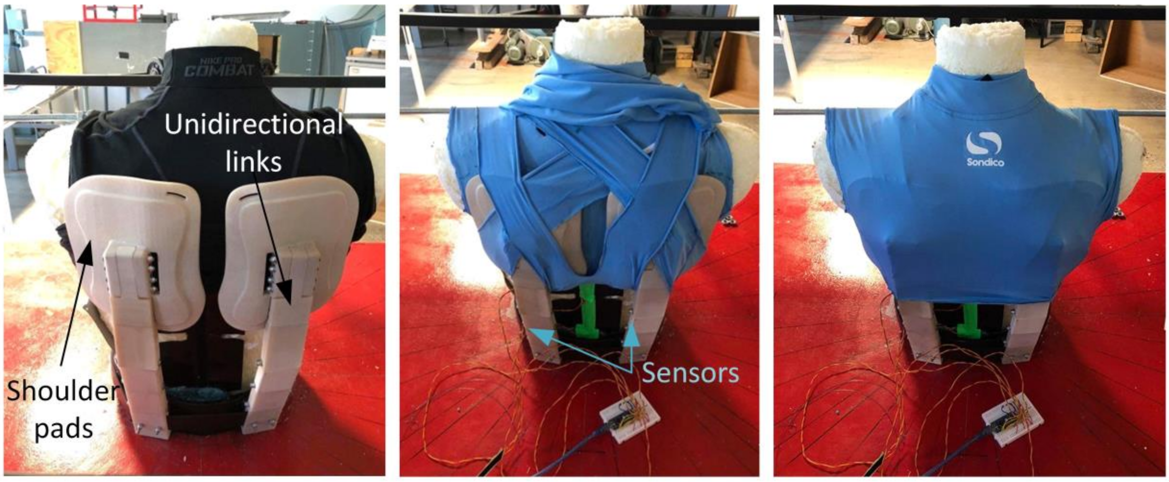

Figure 10 - Assembled 'unidirectional' linked back brace at various stages of attachment

The second design combined the use of a back plate and rods (

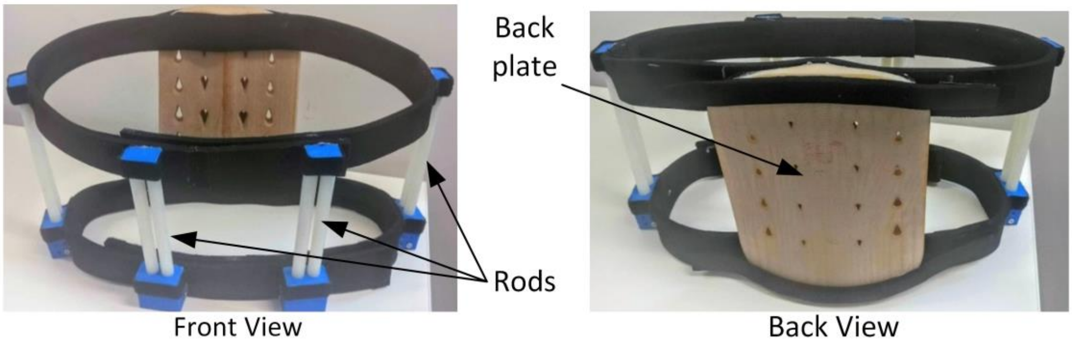

Figure 11). The design intent of this concept was to bridge the gap between the flexible and rigid braces currently available and to restrict flexion, extension and lateral bending in thoracolumbar motion.

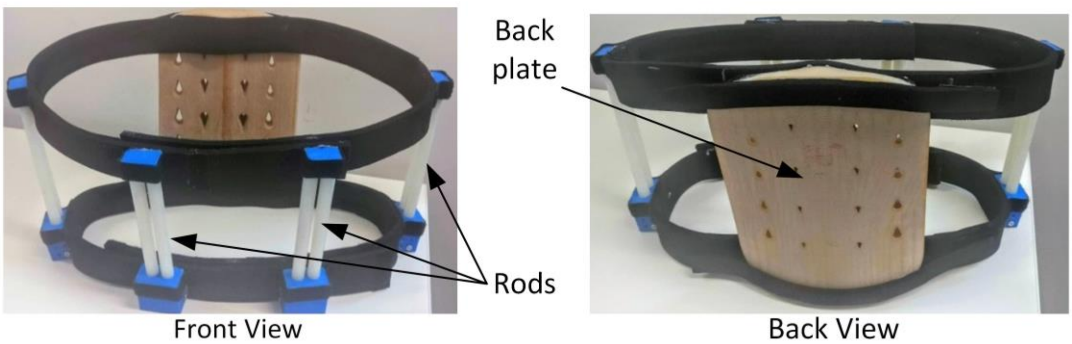

Figure 11 - Assembled combined plate and rod back brace

Test Rig Results

The test rig was used to compare the behaviour of the torso when restricted using back braces and to quantifiably compare back brace design. The two novel designs (rodded and linked) were compared to two commercially available back braces, i.e. a leather weightlifting belt (Gold's Gym) and an lumbar support brace, a back belt with metal splints (TONUS 0012-01 LUX, Tonus Elast). The four braces tested are shown in

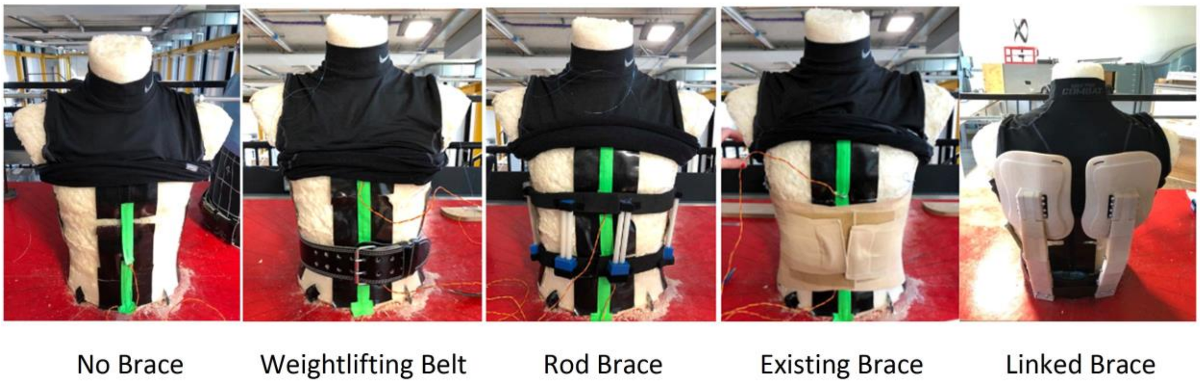

Figure 12, along with the control (no brace).

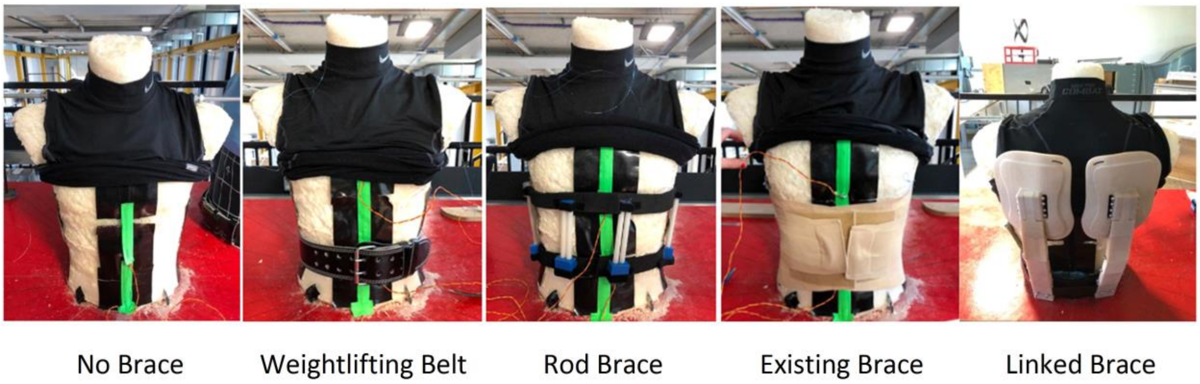

Figure 12 - Overview of brace conditions tested on the rig

Flexion and Extension

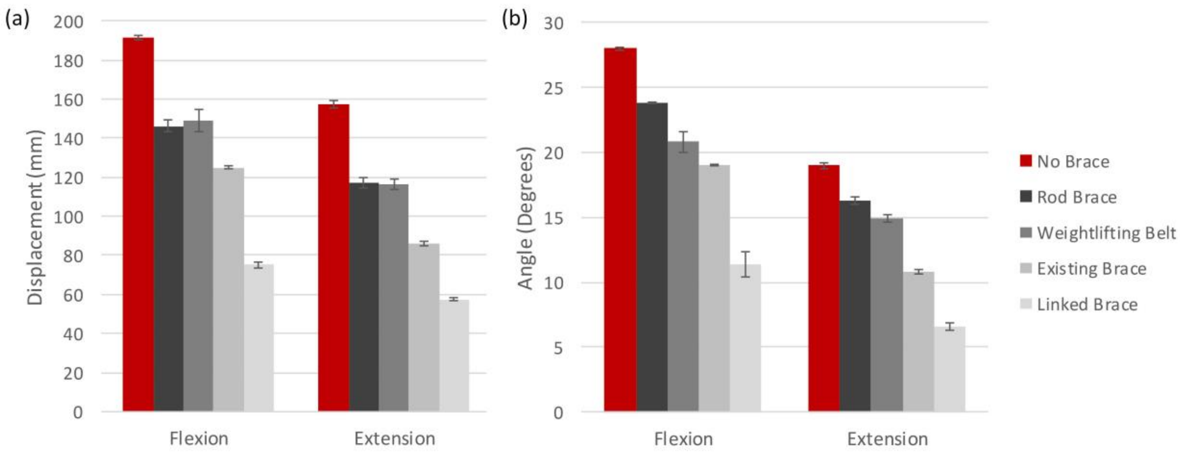

Figure 13 shows how in flexion, the linked brace is by far the most restrictive and the rodded brace the least. As expected, the displacement results show a similar pattern to the measured angles. One noticeable difference between the displacement and angle data is the reduction in flexion for the weightlifting belt – the displacement data shows the belt as restricting flexion by less than the rodded brace, whilst the angle data shows more reduction. The difference in final angle between the weightlifting belt and the rodded brace could be indicative of a shift in the centre of rotation.

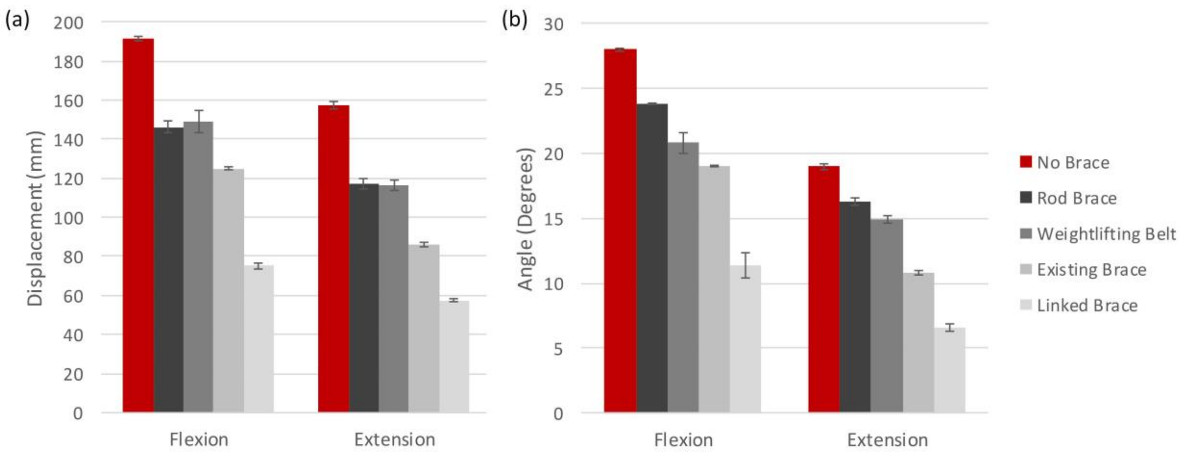

Figure 13 - Comparison of brace motion in flexion and extension. (a) Shows maximum deflection, (b) shows angle of tilt

Lateral Bending

In both cases, lateral bending shows a discrepancy between left and right motion (

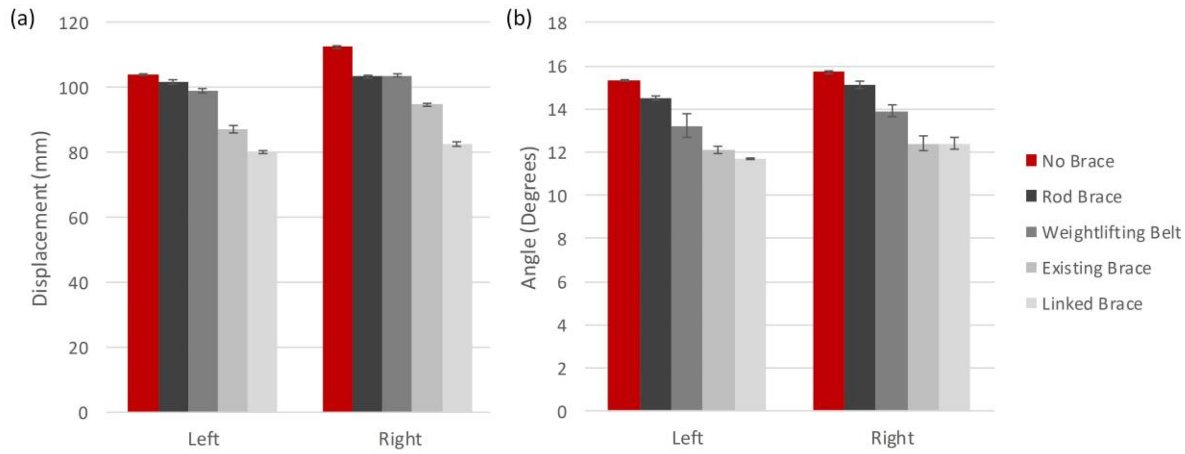

Figure 14). This may be due to inhomogeneous properties of the cast foam in the torso. Of the two designed braces, the rod brace can be seen to restrict the least motion and the linked brace the most.

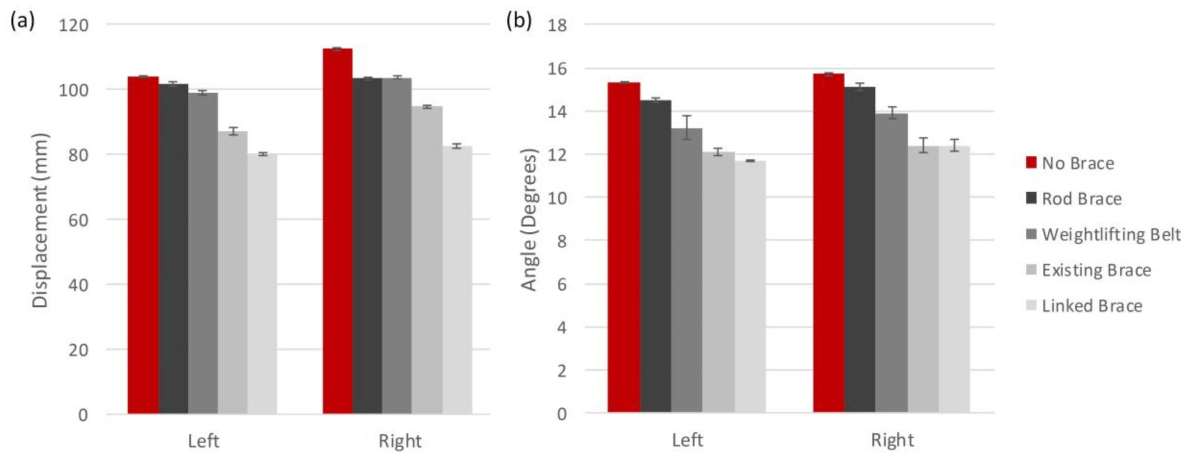

Figure 14 - Comparison of brace motion in lateral bending in both left and right directions. (a) Shows maximum deflection, (b) shows angle of tilt

Torsion

From the outset of this work, it was suspected that torsion would be the most difficult motion to restrict and this has been shown to be true from the results gained. The two designed braces were less effective at reducing torsion, as evidenced in

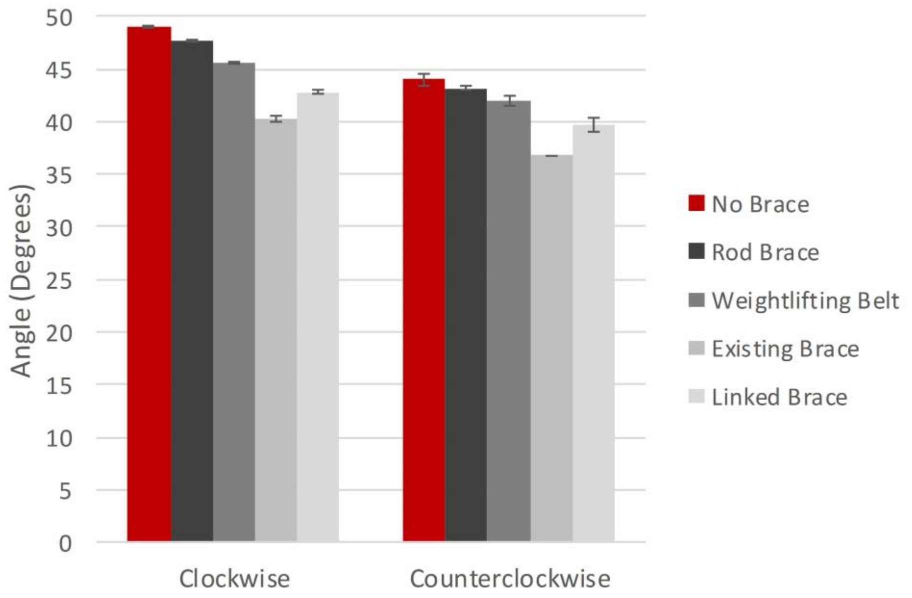

Figure 15. The commercial elastic brace is seen to reduce the most motion, likely due to the larger contact area with the body of the torso.

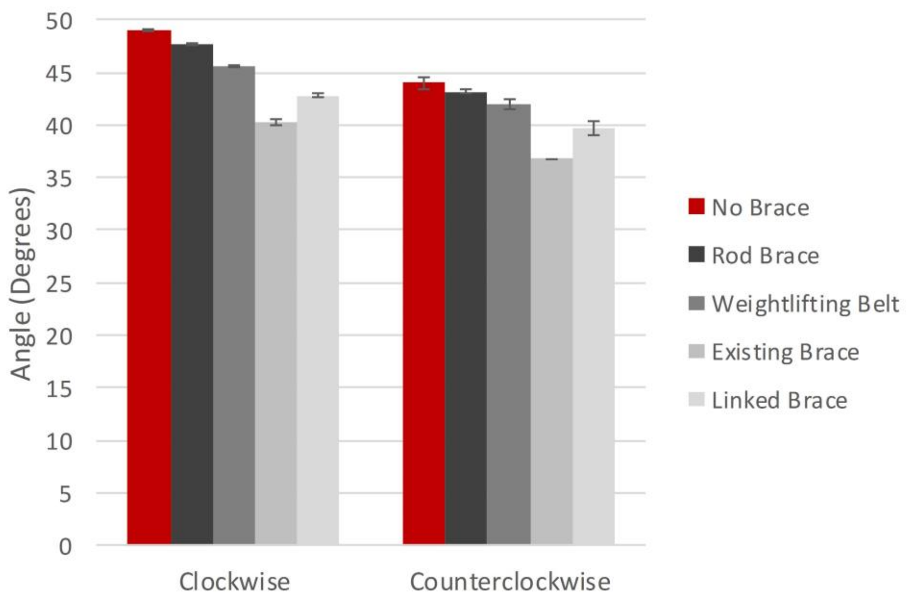

Figure 15 - Comparison of angle of rotation of brace in clockwise and anticlockwise torsion

Conclusion

Here an experimental test rig and finite element simulation has been developed for the first time that mimics the mechanical behaviour of the human torso, with the purpose of facilitating the design of back braces. The test rig and simulation models incorporate a mechanically equivalent artificial spine with geometries and properties that are comparable to those found in human tissues. This allows researchers to test different back brace configurations without having to resort to human testing in the first instance with all the logistical and ethical issues that those tests necessitate. Another advantage of this novel design process is that the back braces can be compared quantifiably in a more convenient manner than in traditional design strategies. It also means that different spine configurations and deformities, such as scoliosis, can be modelled and tested with different back braces without causing any discomfort. It is recognised that ultimately, testing on humans is necessary in order to optimise for factors such as comfort and muscle engagement, but this new design process should facilitate innovation in this field.

Acknowledgments

Competing interests: None declared

Funding: Lancaster University Engineering Department

Ethical approval: Not required

References

An, N., 2014. *Human spine.* [Online] Available at: https://grabcad.com/library/human-spine-1 [Accessed 01 October 2018].

ANSYS, 2017. Workbench - Mechanical Introduction 18.0.

Bayoglu, R. et al., 2019. Twente Spine Model: A thorough investigation of the spinal loads in a complete and coherent musculoskeletal model of the human spine. *Medical engineering & physics,* Volume 68, pp. 35-45.

Bonnaire, R. et al., 2014. Biomechanical analysis and modelling of lumbar belt: parametric study. *Computer Methods in Biomechanics and Biomedical Engineering,* S1(62-63), p. 17.

Carboni, M. & Dal Pozzo, E., 2017. *Integration of muscle forces and gravity loads in a finite element model of the lumbar spine,* s.l.: Master Graduation Thesis, Scuola di Ingegneria Industriale e dell'Informazione Corso di Laurea Magistrale in Ingegneria Biomedica.

Cholewicki, J., McGill, K., Shah, K. R. & Lee, A. S., 2010. The effects of a three-week use of lumbosacral orthoses on trunk muscle activity and on the muscular response to trunk perturbations. *BMC Musculoskeletal Disorders,* Volume 11.

Cholewicki, J., McGill, S. M. & Norman, R. W., 1995. Comparison of muscle forces and joint load from an optimization and EMG assisted lumbar spine model: Towards development of a hybrid approach. *Journal of Biomechanics,* 28(3), pp. 321-331.

Cholewicki, J., Reeves, N. P., Everding, V. Q. & Morrisette, D. C., 2007. Lumbosacral orthoses reduce trung muscle activity in a postural control task. *Journal of Biomechanics,* 40(8), pp. 1731 - 1736.

Dreischarf, M. et al., 2014. Comparison of eight published static finite element models of the intact lumbar spine: predictive power of models improves when combined together. *Journal of Biomechanics,* 47(8), pp. 1757-1766.

Eisinger, D. B., Kumar, R. & Woodrow, R., 1996. Effect of lumbar orthotics on trunk muscle strength. *American Journal of Physical Medicine and Rehabilitation,* 75(3), pp. 194-197.

Fayolle-Minon, I. & Calmels, P., 2008. Effect of wearing a lumbar orthosis on trunk muscles: Study of the muscle strength after 21 days of use on healthy subjects. *Joint Bone Spine,* 75(1), pp. 58-63.

Gómez, F., Lorza, R., Bobadilla, M. & García, R., 2017. Improving the process of adjusting the parameters of finite element models of healthy human intervertebral discs by the multi-response surface method. *Materials,* 10(10), pp. 1116-1154.

Hawkinson, N. V., 2016. *Back Conditions Treated by Spinal Bracing.* [Online] Available at: https://www.spineuniverse.com/treatments/bracing/back-conditions-treated-spinal-bracing

Hoy, D. et al., 2014. The global burden of low back pain: estimates from the Global Burden of Disease 2010 study. *Annals of the Rheumatic Diseases,* 73(6), pp. 968-974.

Hsu, J. D., Michael, J. & Fisk, J., 2008. *AAOS Atlas of orthoses and assistive devices e-book.* s.l.:Elsiever Health Sciences.

Huynh, K. T., Gibson, I. & Gao, Z., 2012. Development of a Detailed Human Spine Model with Haptic Interface. *In Haptics Rendering and Applications. InTech,* pp. 165-194.

Ivancic, P. C., Cholewicki, J. & Radebold, A., 2002. Effects of the abdominal belt on muscle-generated spinal stability and L4/L5 joint compression force. *Ergonomics*, 45(7), pp. 501-513.

Kawaguchi, Y., Gejo, R., Kanamori, M. & Kimura, T., 2002. Quantitative analysis of the effect of lumbar orthosis on trunk muscle strength and mussle activity in normal subjects. *Journal of Orthopaedic Science,* Volume 7, pp. 483-489.

Kurutz, M., 2010. Finite element modelling of human lumbar spine. *Finite Element Analysis. InTech.*

Lariviere, C., Caron, J.-M., Preuss, R. & Mecheri, H., 2014. The effect of different lumbar belt designs on lumbopelvic rhythm in healthy subjects. *BMC Musculoskeletal Disorders,* 15(307).

Longo, U. G. et al., 2012. Conservative management of patients with an osteoporotic vertebral fracture: a review of the literature.. *The Journal of Bone and Joint Surgery,* 94(2), pp. 152-157.

Materialise, N., 2018. *Materialse Mimics.* [Online]
Available at: https://www.materialise.com/en/medical/software/mimics
[Accessed 01 October 2018].

Morl, F. & Bradl, I., 2013. Lumbar posture and muscular activity while sitting during office work. *Journal of electromyography and kinesiology,* 23(2), pp. 362-368.

Office for National Statistics, 2017. *Work-related Musculoskeletal Disorders (WRMSDs) Statistics in Great Britain 2017,* London: Office for National Statistics.

Panjabi, M. et al., 1992. Human lumbar vertebrae. Quantitative three-dimensional anatomy. *Spine,* 17(3), pp. 299-306.

Pitzer, M. et al., 2016. A numerical study to determine the effectof ligament stiffness on kinematics of thelumbar spine during flexion. *BMC Musculoskeletal Disorders,* 17(95).

Rohlmann, A. et al., 2006. Determination of trunk muscle forces for flexion and extension by using a validated finite element model of the lumbar spine and measured in vivo data. *Journal of Biomechanics,* 39(6), pp. 981-989.

Schmidt, H. et al., 2006. Application of a new calibration method for a three-dimensional finite element model of a human lumbar annulus fibrosus. *Clinical Biomechanics,* 21(4), pp. 337-344.

Seo, K., Cho, C. & Hong, S., 2013. Evaluation of the shock absorption properties of rigid polyurethane and polystyrene foam used in a small transport package. *Packaging, Transport, Storage & Security of Radioactive Material,* 16(2), pp. 145-150.

Swamy, A., 2014. Material selection for modeling of intervertebral disc. *Int J Scientific Engineering and Research,* 2(4), pp. 51-53.

Ultimaker, 2017. *Technical data sheet ABS.* [Online]
Available at: http://www.farnell.com/datasheets/2310520.pdf

Wagnac, E. et al., 2011. Calibration of hyperelastic material properties of the human lumbar intervertebral disc under fast dynamic compressive loads. *J Biomech Eng.,* 133(10), p. 101007.

Wang, J. P. et al., 2006. Finite element analysis of the spondylolysis in lumbar spine. *Bio-Medical Materials and Engineering,* 16(5), pp. 301-308.

Woolf, A. & Pfleger, B., 2003. Burden of major musculoskeletal conditions. *Bulletin of the World Health Organization,* Volume 81, pp. 646-656.

Yamamoto, I., Panjabi, M., Crisco, T. & Oxland, T., 1989. Three-dimensional movements of the whole lumbar spine and lumbosacral joint. *Spine*, 14(11), pp. 1256-1260.